Journal of Power Sources 269 (2014) 424–429

Contents lists available at ScienceDirect

Journal of Power Sources

journal homepage: www.elsevier.com/locate/jpowsour

Thermodynamics of high-temperature, high-pressure water electrolysis

Devin Todd, Maximilian Schwager, Walter Mérida*

Clean Energy Research Centre, The University of British Columbia, 2054-6250 Applied Science Lane, Vancouver, BC V6T 1Z4, Canada

HIGHLIGHTS

- We present electrochemical potentials for H_2O electrolysis up to 10^3 K and 10^2 MPa.
- Using advanced property models, errors of common ideal assumptions are quantified.
- Energy analyses study pressurized electrolysis versus product gas compression.

ARTICLE INFO

Article history:
Received 21 March 2014
Accepted 25 June 2014
Available online 7 July 2014

Keywords:
Electrolysis
Supercritical
High temperature
High pressure
Thermodynamics

ABSTRACT

We report on a thermodynamic analysis for water electrolysis from normal conditions ($P = 0.1$ MPa, $T = 298$ K) up to heretofore unaddressed temperatures of 1000 K and pressures of 100 MPa. Thermoneutral and reversible potentials are determined using equations-of-state published by the International Association for the Properties of Water and Steam and the National Institute of Standards and Technology. The need for using accurate property models at these elevated temperatures and pressures is exemplified by contrasting results with those obtained via ideal assumptions. The utility of our results is demonstrated by their application in an analysis comparing pressurized electrolysis versus mechanical gas compression. Within the limits of our analysis, pressurized electrolysis demonstrates lower energy requirements albeit with electrical work composing a greater proportion of the total energy input.

1. Introduction

Hydrogen is expected to play a critical role in future energy systems, by complementing or replacing fossil fuels in numerous applications [1,2]. Beyond its application in electrochemical and combustion systems as a zero-emissions fuel, hydrogen also serves as a feedstock in many industrial chemical processes (e.g., the Fischer-Tropsch processes for liquid hydrocarbon synthesis.) Currently, the largest portion of global hydrogen production involves the reformation of fossil fuels (mostly natural gas). Among the alternative, clean, hydrogen pathways is water electrolysis powered by renewable or other carbon-free sources.

We report on a thermodynamic analysis for water electrolysis from normal conditions ($p = 0.1$ MPa, $T = 298$ K) up to 1000 K and 100 MPa. The reversible and thermoneutral cell potentials as functions of temperature and pressure shall be described, and their utility demonstrated via energy analyses of archetype systems featuring competing pressurization strategies.

Operation outside normal conditions is foreseen to be advantageous in terms of total energy consumption and energy utilization. Elevated temperature decreases the reversible work required to perform electrolysis, making cogeneration in thermal power plants viable [3]. Elevated pressure eliminates the need to compress product gases, at the expense of requiring a pressurized feedwater input. Hence, for an electrolysis plant, the lower energy required for pressurizing the denser water may improve overall efficiency. Additionally are possible reductions in electrochemical overpotentials; improved reaction kinetics, and enhanced mass transport performance especially in the supercritical phase. These overpotentials are however beyond the scope of this work.

Contemporary systems for hydrogen production via electrolysis can be classified, like their fuel cell counterparts, according to the ionic conductor type and the temperature of operation. Proton-exchange membrane electrolysis cells (PEMECs) operate between 70 and 100 °C, alkali cells 80–90 °C, and solid-oxide electrolysis cells (SOECs) at higher temperatures (600–1200 °C) [4–6]; all of which have operating pressures near atmospheric. Experimental

* Corresponding author. Tel.: +1 604 822 4189; fax: +1 604 822 2403.
E-mail address: walter.merida@ubc.ca (W. Mérida).

http://dx.doi.org/10.1016/j.jpowsour.2014.06.144
0378-7753/

efforts have explored the performance outside these conventional envelopes. For example: steam temperatures in proton-exchange membrane (PEM) systems using alternative membranes [7]; and pressurized PEMEC and SOEC systems, having achieved pressures of 7 MPa and 1 MPa respectively [5,6]. Alkaline systems, approaching [10] and in one case exceeding supercritical water conditions [11] have been reported.

Theoretical treatments that are complementary to experimental efforts are available. In an attempt to remedy perceived inaccuracies in the literature of the time, Leroy et al. calculated theoretical potentials for alkaline electrolysis in the ranges of 25–250 °C and 1–100 atm [12]. The expressions for enthalpies considered real gases, but ideal mixtures; whereas expressions for Gibbs free energy (and thus reversible potential) treated all species as ideal. The implications of different systems level operating strategies were not addressed. Onda et al. calculated theoretical potentials for (non-specific) electrolysis in the ranges of 25–250 °C and 1–700 atm [13]; applying these to high-pressure electrolysis systems analysis. Their work followed the expressions developed by Leroy, though with a different source for reference pressure properties as a function of temperature.

In the present study we address current challenges and knowledge gaps of the literature by: expanding the parameter ranges considered, incorporating advanced property models, demonstrating the error when inappropriate models are implemented, and analysing electrolysis configurations operating at the extremes of the ranges.

2. Method

The treatment assumes a reversibly operated electrolysis cell (i.e. without overpotentials); where the inlet stream is pure water of a single phase at prescribed pressure and temperature. The two independent outlet streams are pure hydrogen and oxygen at the same pressure and temperature. This is shown schematically in Fig. 1. The full and half-cell reactions for an (acid electrolyte) electrolysis cell are:

$$H_2O \rightarrow 0.5O_2 + 2e^- + 2H^+ \quad \text{anode} \tag{1}$$

$$2H^+ + 2e^- \rightarrow H_2 \quad \text{cathode} \tag{2}$$

$$H_2O \rightarrow H_2 + 0.5O_2 \quad \text{cell} \tag{3}$$

The net energy input (work & heat) required is given by the 1st law of thermodynamics. Neglecting potential, kinetic and other terms, it may be expressed for a control volume (CV) encompassing the cell operating at steady-state:

$$\frac{dE_{cv}}{dt} = 0 = \dot{Q} - \dot{W} + \dot{n}_{H_2O}\tilde{h}_{(H_2O|p,T)} - \dot{n}_{H_2}\tilde{h}_{(H_2|p,T)} - \dot{n}_{O_2}\tilde{h}_{(O_2|p,T)} \tag{4}$$

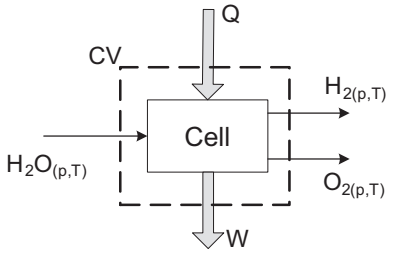

Fig. 1. System schematic.

where $\tilde{h}_{i|p,T}$ denotes molar enthalpy at temperature T and pressure p for species i. Rearranging and scaling terms per coulomb of charge transferred yields:

$$E_{th} = \frac{\dot{W} - \dot{Q}}{\dot{n}_{H_2} nF} = \frac{\tilde{h}_{(H_2O|p,T)} - \tilde{h}_{(H_2|p,T)} - 0.5\tilde{h}_{(O_2|p,T)}}{nF} \tag{5}$$

where E_{th} is the thermoneutral cell potential.

The reversible work input required is obtained by substituting the 2nd law of thermodynamics for the $\dot{Q}$ term of Eq. (4). What follows is an expression involving the Gibbs free energies of the species:

$$\dot{W} = \dot{n}_{H_2O}\left(\tilde{h}_{(H_2O|p,T)} - T\tilde{s}_{(H_2O|p,T)}\right) - \dot{n}_{H_2}\left(\tilde{h}_{(H_2|p,T)} - T\tilde{s}_{(H_2|p,T)}\right) - \dot{n}_{O_2}\left(\tilde{h}_{(O_2|p,T)} - T\tilde{s}_{(O_2|p,T)}\right) \tag{6}$$

Rewriting the equation per coulomb of charge transferred yields the reversible cell potential.

$$E_{rev,cell} = \frac{\dot{W}}{\dot{n}_{H_2} nF} = \frac{\tilde{g}_{(H_2O|p,T)} - \tilde{g}_{(H_2|p,T)} - 0.5\tilde{g}_{(O_2|p,T)}}{nF} \tag{7}$$

The quality of a (thermo analysis) model is contingent on the accuracy of supporting data. This work makes use of the most recent equations-of-state (EOS) for thermodynamic properties recognized by: the International Association for the Properties of Water and Steam (IAPWS), the National Institute of Standards and Technology (NIST), and the International Council for Science : Committee on Data for Science and Technology (CODATA). More specifically, the following sources are used:

- For water, this analysis uses the IAPWS 1995 release on the properties of ordinary water, as implemented in the WATER95 MATLAB library [14,15]. IAPWS-95 describes water over the ranges of the melting pressure curve to 1273 K at 1000 MPa, though this may be extended to 100 GPa and 5000 K.
- For (normal) hydrogen, this analysis uses an expression developed by Leachman et al., valid up to 1000 K and 2000 MPa [16].
- For oxygen, this analysis uses an expression developed by Schmidt and Wagner [17]. Originally conceived for an upper limit of 300 K and 818 bar, it may be extrapolated with accuracy to 1000 K and 100 MPa [18].
- For translation of the aforementioned data to a consistent reference frame, this analysis uses standard-state enthalpy of formation and entropy from CODATA Key Values for Thermodynamics [19].

The aforementioned equations-of-state describe succinctly the thermodynamic properties of their respective fluids via two-part expressions for non-dimensional Helmholtz free energy as a function of reduced density and reduced inverse temperature (Eq. (8)).

$$\phi(\delta,\tau) = \phi^0(\delta,\tau) + \phi^r(\delta,\tau) \quad \text{where}: \phi = \frac{a}{RT} \quad \delta = \frac{\rho}{\rho_c} \quad \tau = \frac{T_c}{T} \tag{8}$$

Such description is advantageous as it does not require ancillary equations (e.g.: is not susceptible to errors from multiple equation incongruities). Appropriate partial derivatives of the ideal and residual Helmholtz free energy components yield the necessary parameters (Eqs. (9)–(11)).

$$p = \rho RT\left[1 + \delta\left(\frac{\partial \phi^r}{\partial \delta}\right)_\tau\right] \tag{9}$$

$$\frac{h}{RT} = \tau\left[\left(\frac{\partial \phi^0}{\partial \tau}\right)_\delta + \left(\frac{\partial \phi^r}{\partial \tau}\right)_\delta\right] + \delta\left(\frac{\partial \phi^r}{\partial \delta}\right)_\tau + 1 \tag{10}$$

$$\frac{s}{R} = \tau\left[\left(\frac{\partial \phi^0}{\partial \tau}\right)_\delta + \left(\frac{\partial \phi^r}{\partial \tau}\right)_\delta\right] - \phi^0 - \phi^r \tag{11}$$

To emphasize the importance of considering real thermodynamic properties, reversible and thermoneutral cell potentials are also calculated using ideal (but non-perfect) assumptions. For this scenario, if the water is in liquid phase, real IAPWS data are used. Otherwise water, hydrogen and oxygen enthalpies and Gibbs free energies are calculated per Eqs. (12) and (13):

$$h(p,T) = h\left(p_{\text{ref}}, T\right) \tag{12}$$

$$\begin{aligned} g(p,T) &= h\left(p_{\text{ref}}, T\right) - Ts(p,T) \\ &= h\left(p_{\text{ref}}, T\right) - T\left(s\left(p_{\text{ref}}, T\right) - Rln\left(\frac{p}{p_{\text{ref}}}\right)\right) \end{aligned} \tag{13}$$

where enthalpy and entropy as functions of temperature at reference pressure are calculated from NIST/IAPWS data; whilst CODATA data are again used for setting the species independent reference frame.

The second part of this work is a limited investigation of two illustrative strategies for obtaining product gas in a compressed state. The first strategy (A) operates an electrolysis cell in a pressurized state by running feedwater through a pump. The second (B) operates an electrolysis cell at atmospheric pressure with subsequent mechanical compression of product gases (including the oxygen). Provisions are allowed to accommodate elevated operating temperature. The two configurations are presented in Fig. 2.

The gas and water compressors are taken as adiabatic and isentropic. Eq. (14) expresses the work flux for these devices.

$$\dot{W}_{1\to 2}^{\text{compressor}} = \dot{n}_i\left(\tilde{h}_{(i|p_1,T)_1} - \tilde{h}_{(i|p_2,T_2)}\right), \quad \text{where}: \tilde{s}_{(i|p_1,T_1)} = \tilde{s}_{(i|p_2,T_2)} \tag{14}$$

The heat exchange elements regulate temperatures prior to the electrolyser and cool product gases. To reduce complexity; heating is taken as an energy requirement into the system, whereas cooling occurs freely to the surroundings (i.e.: no economizers or similar thermal energy recovery systems). Eq. (15) expresses the heat flux for these devices.

$$\dot{Q}_{1\to 2} = \dot{n}_i\left(\tilde{h}_{(i|p_1,T_2)} - \tilde{h}_{(i|p_1,T_1)}\right) \tag{15}$$

Work and total energy potentials are calculated for each strategy. These are the energy fluxes scaled to per coulomb charge transferred. The work comprises contributions from the compressors and the electrolysis reaction. The total energy includes this work and contributions from external heat and the endothermic component of electrolysis. These calculated following Eqs. (16)–(19).

$$\begin{aligned} E_{\substack{\text{work} \\ \text{strategy A}}} &= \frac{\tilde{g}_{(H_2O|A_3)} - \tilde{g}_{(H_2|A_4)} - 0.5\tilde{g}_{(O_2|A_4)}}{nF} \\ &\quad + \frac{\tilde{h}_{(H_2O|A_1)} - \tilde{h}_{(H_2O|A_2)}}{nF} \end{aligned} \tag{16}$$

$$\begin{aligned} E_{\substack{\text{total} \\ \text{strategy A}}} &= \frac{\tilde{h}_{(H_2O|A_3)} - \tilde{h}_{(H_2|A_4)} - 0.5\tilde{h}_{(O_2|A_4)}}{nF} \\ &\quad + \frac{\tilde{h}_{(H_2O|A_1)} - \tilde{h}_{(H_2O|A_2)}}{nF} - \frac{\tilde{h}_{(H_2O|A_3)} - \tilde{h}_{(H_2O|A_2)}}{nF} \end{aligned} \tag{17}$$

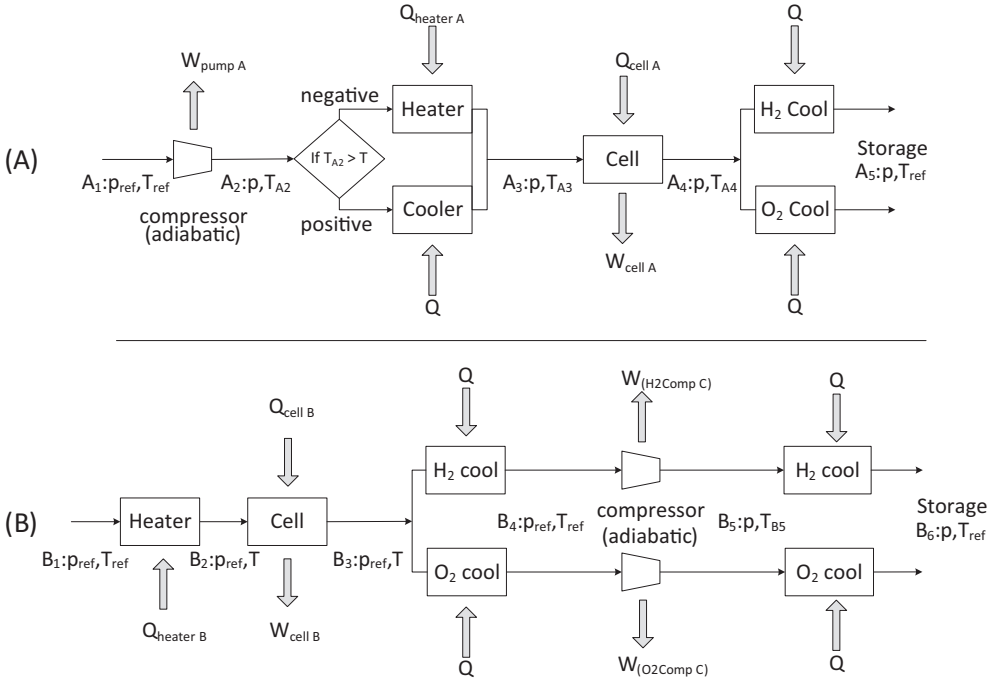

Fig. 2. System schematics. Above: pressurized electrolysis system. Below: ambient pressure electrolysis with adiabatic mechanical product compression.

$$E_{\substack{\text{work}\\ \text{stragegy B}}} = \frac{\tilde{g}_{(H_2O|B_2)} - \tilde{g}_{(H_2|B_3)} - 0.5\tilde{g}_{(O_2|B_3)}}{nF} + \frac{\tilde{h}_{(H_2|B_4)} - \tilde{h}_{(H_2|B_5)}}{nF} + \frac{\tilde{h}_{(O_2|B_4)} - \tilde{h}_{(O_2|B_5)}}{2nF} \quad (18)$$

$$E_{\substack{\text{total}\\ \text{strategy B}}} = \frac{\tilde{h}_{(H_2O|B_2)} - \tilde{h}_{(H_2|B_3)} - 0.5\tilde{h}_{(O_2|B_3)}}{nF} + \frac{\tilde{h}_{(H_2|B_4)} - \tilde{h}_{(H_2|B_5)}}{nF} + \frac{\tilde{h}_{(O_2|B_4)} - \tilde{h}_{(O_2|B_5)}}{2nF} - \frac{\tilde{h}_{(H_2O|B_2)} - \tilde{h}_{(H_2O|B_1)}}{nF} \quad (19)$$

3. Results and discussion

The thermoneutral and reversible cell potentials are plotted as a function of temperature for several pressures in Fig. 3. Analogously, thermoneutral and reversible cell potentials are plotted as a function of pressure for several temperatures in Fig. 4. Note the conformance to IUPAC conventions (where the potential of an electrolytic cell is negative).

As temperature increases, the reversible potential decreases in magnitude. The required work is being offset by the thermal energy contribution to the reaction; which is the difference of the reversible and thermoneutral potentials, and generally increases with temperature. The trend of the total energy requirement (thermoneutral potential) with temperature is pressure dependent; with lower pressures yielding increases in magnitude as temperatures increases, and the inverse for higher pressures. The discontinuities in thermoneutral potential, attributable to feedwater being delivered as either liquid or gaseous, are present because this analysis does not include the process steps of taking water (at arbitrary conditions) to specified pressure and temperature.

As system pressure increases, the reversible potential increases in magnitude; most pronounced for the first few pressure increments. The change in thermoneutral potential as pressure increases is less intuitive. At lower temperatures (e.g.: 298 K), the magnitude first decreases then increases; whereas at higher temperatures, the thermoneutral potential increases in magnitude monotonically.

Comparing reversible and thermoneutral potentials; we observe a substantial increase in the work input required for electrolysis (to jump say 99 bar from 1 bar), whilst the net energy requirement changes only marginally. This suggests a shift occurs in the distribution of energy input requirements, from thermal (heat) to electrical (work). This phenomenon is illustrated in Fig. 5, which plots the ratio of reversible and thermoneutral potentials (equivalent to the percent work in the net energy for electrolysis). Such behaviour is not however consistent over the entire analysis range. At higher pressures and temperatures (say increasing from 700 to 900 bar at 800 K); the increase in work needed is smaller and similar in magnitude to the change in total energy necessary. Here, the electrical versus thermal balance is shifting back towards thermal. Had ideal gas assumptions been made, as is prevalent in the

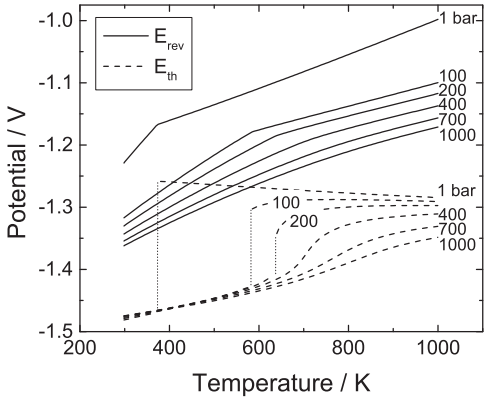

Fig. 3. Thermoneutral and reversible cell potentials plotted vs. temperature for various pressures.

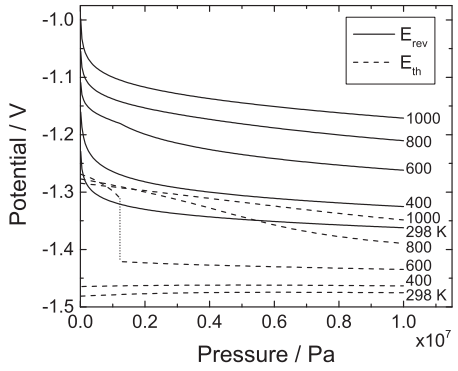

Fig. 4. Thermoneutral and reversible cell potentials plotted vs. pressure for various temperatures.

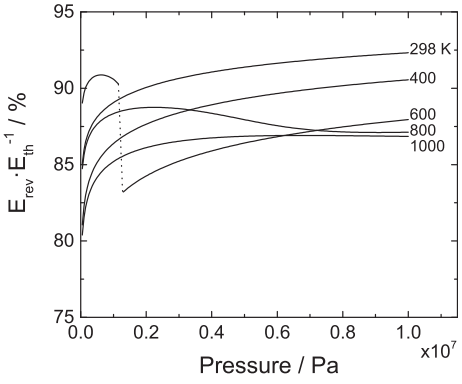

Fig. 5. Reversible work as a percentage of total energy into cell vs. pressure.

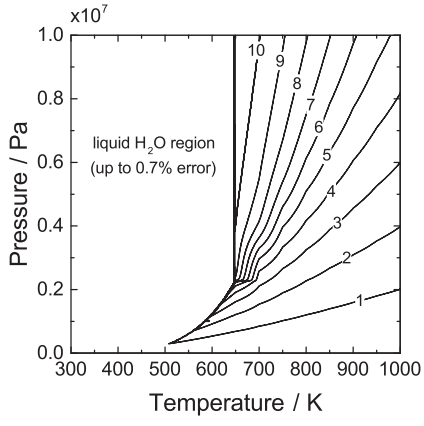

Fig. 6. Contour plot of percent error in thermoneutral cell potential vs. pressure and temperature.

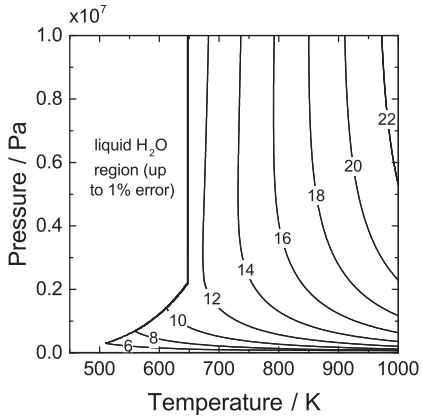

Fig. 7. Contour plot of percent error in reversible cell potential vs. pressure and temperature.

literature, enthalpy being a function of temperature alone would have failed to reveal these behaviours.

Finally, to emphasise the need to consider real species properties when performing thermodynamic calculations at elevated pressures and temperatures; contour plots of the percent error in thermoneutral and reversible cell potentials with ideal assumptions for gas species are presented in Figs. 6 and 7. The error in the thermoneutral and reversible cell potentials with ideal assumptions for gaseous species are greater than 10% and 22% over the investigated range of pressure and temperature. Under conditions where water is in a liquid state, the error is less as real water data are used. Were the additional simplification of perfect gas (i.e.: constant specific heats) behaviour been made, even greater error would be expected as enthalpy and entropy would not track accurately with temperature. Incorrect determination of thermoneutral and reversible potentials can impact directly cell performance predictions; at the limits of our temperature and pressure (and ignoring irreversibilities), the 22% error in reversible potential would yield an approximate 7.2 kW h overestimate in the electricity required to produce 1 kg of hydrogen.

Energy requirements for strategies A and B for product gas synthesis and compression are presented. These are reported as total energy and work potentials, which are analogous to reversible and thermoneutral potentials of the electrolysis cell; but with the inclusion of fluid compression and heating contributions. These potentials are plotted in Fig. 8.

Both the total energy and work requirements are consistently lower (at a given temperature and storage pressure) for pressurized electrolysis (A) versus ambient pressure electrolysis (B) followed by mechanical gas compression. The total energy premium for operating strategy A at progressively higher pressures is miniscule compared to that of strategy B. In fact, studying the sub-critical temperature curves of 298 or 400 K from (a) in Fig. 8, a minimum is observed as pressure increases. The total energy for B as a function of pressure is defined exclusively by increasing compressor work, as both heating and electrolysis occurs at reference pressure.

Examining the percent ratio of work and total potentials, illustrated in Fig. 9, reveals strategy A consistently requires a greater fraction of its energy input as work versus strategy B. Though the

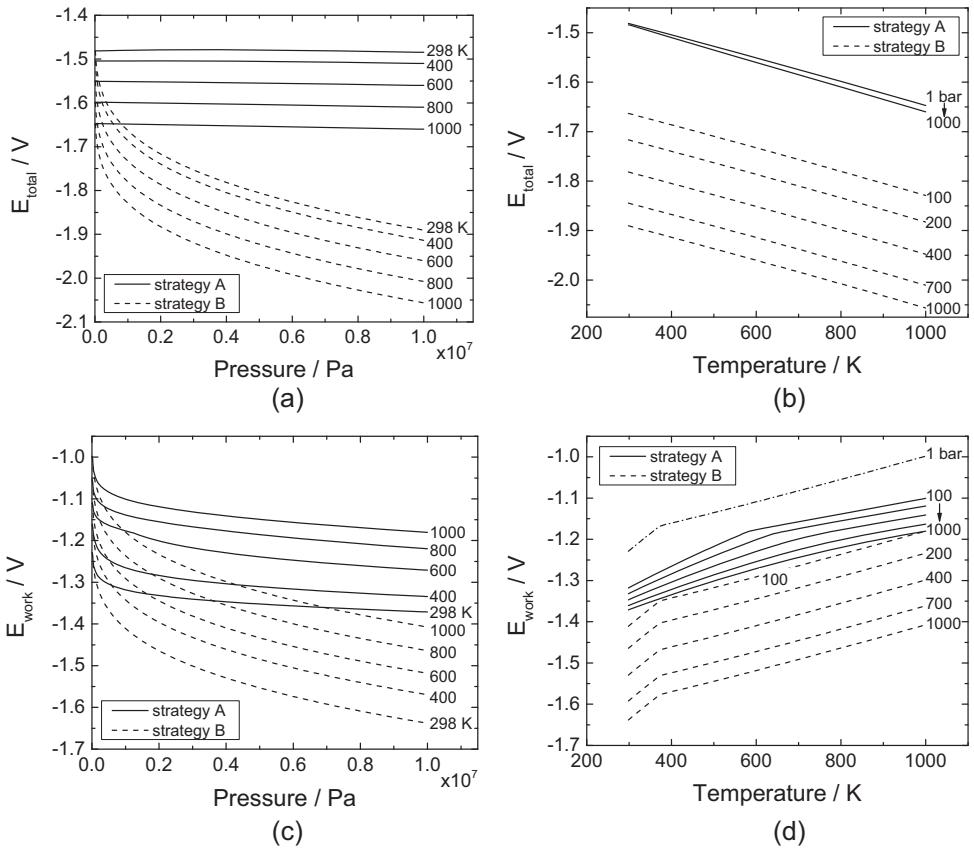

Fig. 8. Work and total energy potentials for competitive production strategies A and B. Negative potentials increasing in magnitude represent greater energies delivered into a system. (a) Total as a function of pressure for select temperatures. (b) Total as a function of temperature for select pressures. (c) Work as a function of pressure for select temperatures. (d) Work as a function of temperature for select pressures.

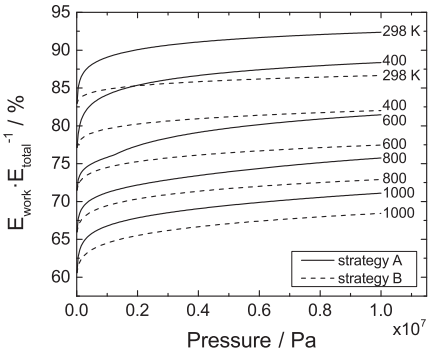

Fig. 9. Percent ratio of work and total energy potentials for production strategies A and B as a function of pressure.

integration with thermal facilities is an associated benefit of high temperature electrolysis (as suggested by the decreasing ratios with temperature); its viability should also consider electrolysis pressure. The difference between strategy A and B, and therefore the need to consider operating pressure, is more pronounced at lower temperatures; where an electrolysis system might otherwise be considered fit for a bottoming cycle in a thermal power plant. This conclusion would only be strengthened for real electrolysis systems, because electrical energy expended into overpotentials and converted to heat would further reduce the window for integrating external heat sources.

4. Conclusion

The reversible and thermoneutral cell potentials for water electrolysis were determined for temperatures and pressures up to 1000 K and 100 MPa respectively. The potentials were obtained with sophisticated real thermodynamic data based on expressions for species Helmholtz free energy. For the conditions investigated, the error of contemporary literature which makes use of ideal thermodynamics relationships was shown to be as large as 22%.

Applying these results in an investigation of archetype electrolysis plants, featuring either pressurized electrolysis or post-electrolysis gas compression, the energy requirements were determined over a heretofore unaddressed operating range of pressure and temperature. Within the scope of this study, pressurized electrolysis required consistently smaller work and total (work and heat) energy inputs. Further, the percentage of work composing total energy for pressurized electrolysis was also greater; suggesting the prospects of integrating an electrolysis system with external thermal sources needs consider both operating temperature and product pressurization strategy (be it electrochemical or mechanical). Ultimately, a design would be driven by the quantity and quality of available energy sources.

References

[1] L. Barreto, A. Makihira, K. Riahi, Int. J. Hydrogen Energy 28 (2003) 267.
[2] C.J. Winter, J. Nitsch, Hydrogen as an Energy Carrier: Technologies, Systems, Economy, Springer-Verlag New York Inc, New York, NY, 1988.
[3] W. Doenitz, R. Schmidberger, E. Steinheil, R. Streicher, Int. J. Hydrogen Energy 5 (1980) 55.
[4] S.C. Singhal, K. Kendall, High Temperature Solid Oxide Fuel Cells: Fundamentals, Design, and Applications, Elsevier Science Ltd, 2003.
[5] A. Hauch, S.D. Ebbesen, S.H. Jensen, M. Mogensen, J. Mater. Chem. 18 (2008) 2331.
[6] K. Zeng, D. Zhang, Prog. Energy Combust. Sci. 36 (2010) 307.
[7] D. Aili, M.K. Hansen, C. Pan, Q. Li, E. Christensen, J.O. Jensen, N.J. Bjerrum, Int. J. Hydrogen Energy 36 (2011) 6985.
[10] J.C. Ganley, Int. J. Hydrogen Energy 34 (2009) 3604.
[11] H. Boll, E.U. Franck, H. Weingärtner, J. Chem. Thermodyn. 35 (2003) 625.
[12] R.L. Leroy, C.T. Bowen, D.J. Eroy, J. Electrochem. Soc. 127 (1980) 1954.
[13] K. Onda, T. Kyakuno, K. Hattori, K. Ito, J. Power Sources 132 (2004) 64.
[14] Revised Release on the IAPWS Formulation 1995 for the Thermodynamic Properties of Ordinary Water Substance for General and Scientific Use, 2009. Doorwerth, The Netherlands.
[15] P. Junglas, Implementing the IAPWS-95 Standard in MATLAB®, 2008.
[16] J.W. Leachman, R.T. Jacobsen, S.G. Penoncello, E.W. Lemmon, J. Phys. Chem. Ref. Data 38 (2009) 721.
[17] R. Schmidt, W. Wagner, Fluid Phase Equilib. 19 (1985) 175.
[18] E.W. Lemmon, R.T. Jacobsen, S.G. Penoncello, D.G. Friend, J. Phys. Chem. Ref. Data 29 (2000) 331.
[19] J.D. Cox, D.D. Wagman, V.A. Medvedev, CODATA Key Values for Thermodynamics, 1989. New York, NY.

Nomenclature

T: temperature, K
p: pressure, Pa
T_{ref}: reference temperature, 298.1 K
p_{ref}: reference pressure, 1×10^5 Pa
ρ: density, mol m^{-3}
$\dot{n}$: mole flux, mol s^{-1}
$\tilde{h}$: molar enthalpy, J mol^{-1}
$\tilde{s}$: molar entropy, J K^{-1} mol^{-1}
$\tilde{g}$: molar Gibbs free energy, J mol^{-1}
$\tilde{a}$: molar Helmholtz free energy, J mol^{-1}
ψ: molar exergy, J mol^{-1}
$\dot{Q}$: heat flux (inwards + ve), J s^{-1}
$\dot{W}$: work flux (outwards + ve), J s^{-1}
E_{rev}: reversible cell potential, V
E_{th}: thermoneutral cell potential, V
n: number of electrons, 2 e^-
F: Faraday constant, 96485 C mol^{-1}
R: ideal gas constant, (function of EOS, 8.314 for ideal calculations) J K^{-1} mol^{-1}
τ: inverse reduced temperature, dimensionless
φ: non-dimensional Helmholtz free energy, dimensionless
δ: reduced density, dimensionless
$Subscript_c$: supercritical-point property, –
$Superscript^0$: ideal component, –
$Superscript^r$: residual component. –

Update

Journal of Power Sources

Volume 289, Issue , 1 September 2015, Page 184–186

DOI: https://doi.org/10.1016/j.jpowsour.2015.04.161

Journal of Power Sources 289 (2015) 184–186

Contents lists available at ScienceDirect

Journal of Power Sources

journal homepage: www.elsevier.com/locate/jpowsour

Corrigendum

Corrigendum to "Thermodynamics of high-temperature, high-pressure water electrolysis" [J. Power Sources (2014) 424–429]

Devin Todd, Maximilian Schwager, Walter Mérida*

Clean Energy Research Centre, The University of British Columbia, 2054-6250 Applied Science Lane, Vancouver BC V6T 1Z4, Canada

The authors regret having incorrectly labelled the Pressure axes of Figs. 4–7, 8a, 8c and 9.

The original manuscript illustrates pressures peaking at 1×10^7 Pa. This should have been 1×10^8 Pa; consistent with the peak pressures illustrated on other figures.

We confirm the discrepancy is restricted to the *labelling* of axes, the underlying data is correct and unchanged.

We have included in this document revised versions of the aforementioned figures with Pressure axes labels of 0×10^5 to 1000×10^5 Pa.

The authors would like to apologise for any inconvenience caused.

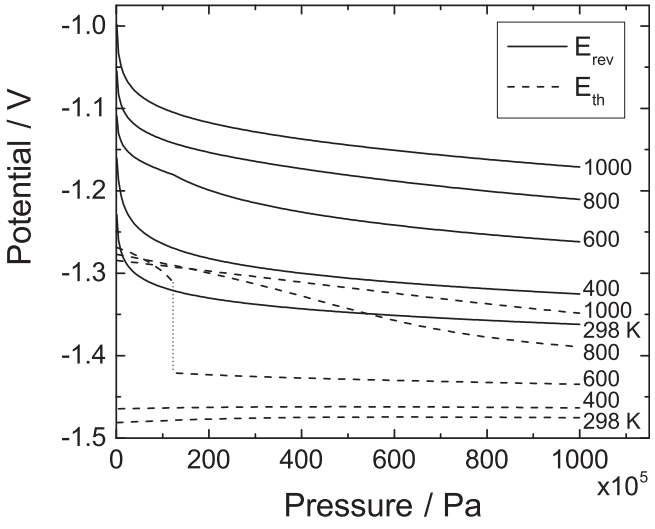

Fig. 4. Thermoneutral and reversible cell potentials plotted vs. pressure for various temperatures.

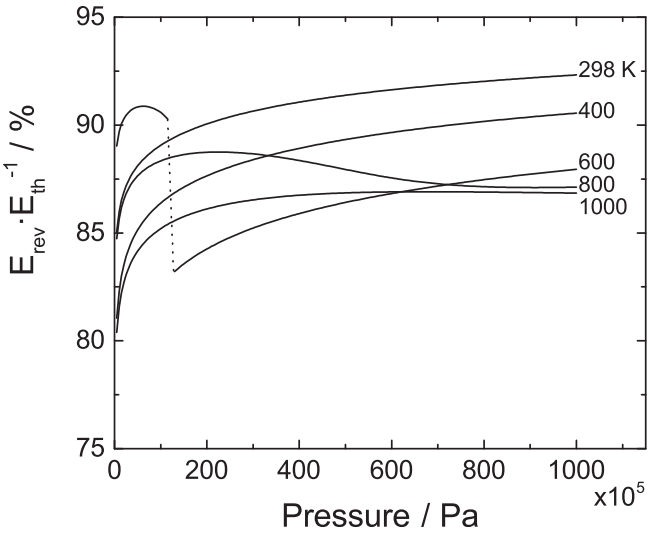

Fig. 5. Reversible work as a percentage of total energy into cell vs. pressure.

DOI of original article: http://dx.doi.org/10.1016/j.jpowsour.2014.06.144.

* Corresponding author.
E-mail address: walter.merida@ubc.ca (W. Mérida).

http://dx.doi.org/10.1016/j.jpowsour.2015.04.161

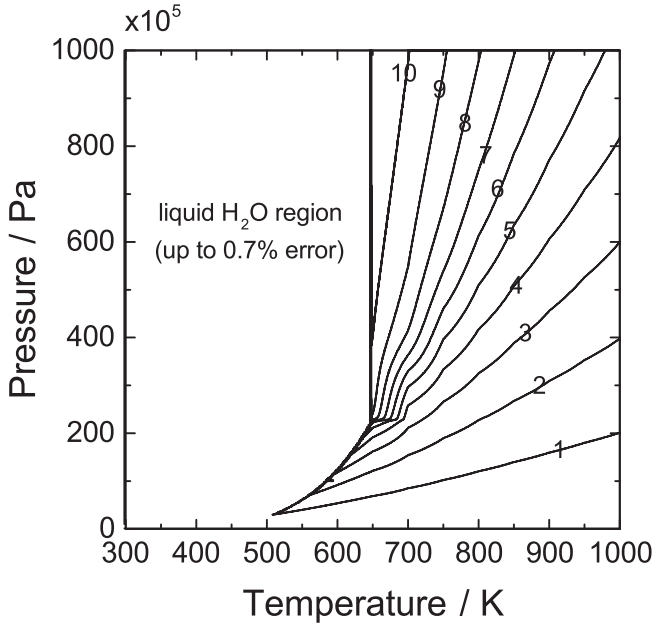

Fig. 6. Contour plot of percent error in thermoneutral cell potential vs. pressure and temperature.

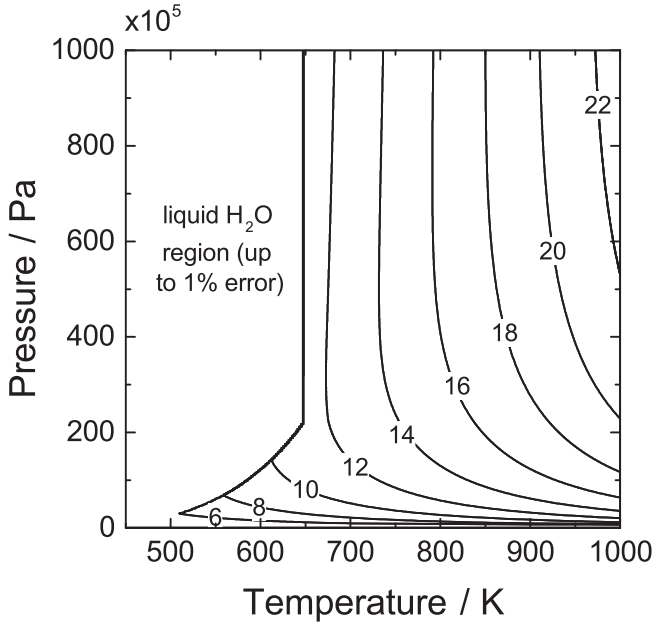

Fig. 7. Contour plot of percent error in reversible cell potential vs. pressure and temperature.

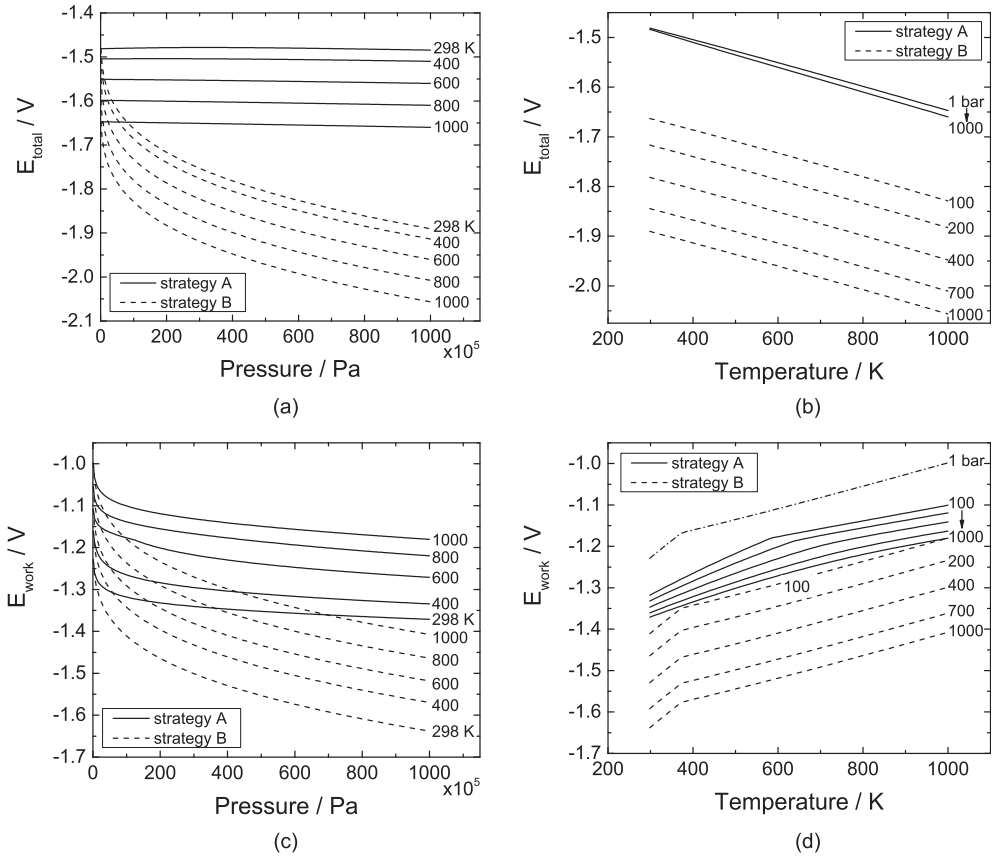

Fig. 8. Work and total energy potentials for competitive production strategies A and B. Negative potentials increasing in magnitude represent greater energies delivered into a system. (a) total as a function of pressure for select temperatures. (b) total as a function of temperature for select pressures. (c) work as a function of pressure for select temperatures. (d) work as a function of temperature for select pressures.

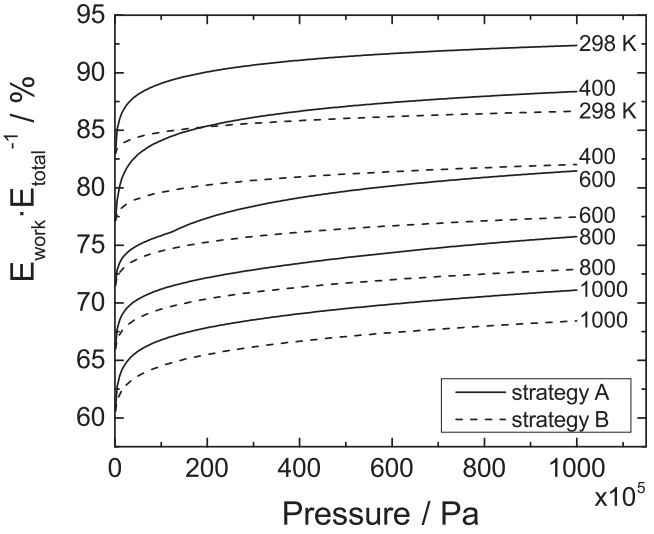

Fig. 9. Percent ratio of work and total energy potentials for production strategies A and B as a function of pressure.